nature chemical biology

Novel targets for Huntington's disease in an mTOR-independent autophagy pathway

Andrea Williams[1,6], Sovan Sarkar[1,6], Paul Cuddon[1,2,6], Evangelia K Ttofi[1,3], Shinji Saiki[1], Farah H Siddiqi[1], Luca Jahreiss[1], Angeleen Fleming[2], Dean Pask[2], Paul Goldsmith[4], Cahir J O'Kane[3], Rodrigo Andres Floto[5] & David C Rubinsztein[1]

Autophagy is a major clearance route for intracellular aggregate-prone proteins causing diseases such as Huntington's disease. Autophagy induction with the mTOR inhibitor rapamycin accelerates clearance of these toxic substrates. As rapamycin has nontrivial side effects, we screened FDA-approved drugs to identify new autophagy-inducing pathways. We found that L-type Ca^{2+} channel antagonists, the K^+_{ATP} channel opener minoxidil, and the G_i signaling activator clonidine induce autophagy. These drugs revealed a cyclical mTOR-independent pathway regulating autophagy, in which cAMP regulates IP_3 levels, influencing calpain activity, which completes the cycle by cleaving and activating $G_{s\alpha}$, which regulates cAMP levels. This pathway has numerous potential points where autophagy can be induced, and we provide proof of principle for therapeutic relevance in Huntington's disease using mammalian cell, fly and zebrafish models. Our data also suggest that insults that elevate intracytosolic Ca^{2+} (like excitotoxicity) inhibit autophagy, thus retarding clearance of aggregate-prone proteins.

The autophagy-lysosomal and ubiquitin-proteasome pathways are major routes for protein and organelle clearance in eukaryotic cells. While the narrow pore of the proteasome barrel precludes clearance of large membrane proteins and protein complexes (including oligomers and aggregates), mammalian lysosomes can degrade protein complexes and organelles by macroautophagy, generally referred to as autophagy[1]. It involves the formation of double membrane structures called autophagosomes around a portion of cytosol. These fuse with lysosomes where their contents are degraded. Autophagy can be induced by several conditions, including starvation, and it is regulated by a number of protein kinases, the best characterized being the mammalian target of rapamycin (mTOR)[2].

Autophagy induction may represent a tractable therapeutic strategy for neurodegenerative disorders caused by aggregate-prone intracytosolic proteins, including Huntington's disease (HD), an autosomal-dominant neurodegenerative disorder caused by a CAG trinucleotide repeat expansion (>35 repeats), which encodes an abnormally long polyglutamine (polyQ) tract in the N terminus of the huntingtin protein[1,3]. Mutant huntingtin toxicity is thought to be exposed after the protein is cleaved to form N-terminal fragments comprising the first 100–150 residues with the expanded polyQ tract, which are also the toxic species found in aggregates and inclusions[3]. Thus, HD pathogenesis is frequently modeled with exon 1 fragments containing expanded polyQ repeats, which cause aggregate formation and toxicity in cell models and *in vivo*[3] (**Supplementary Fig. 1a** online). The polyQ mutation in HD raises intracellular calcium (Ca^{2+}) levels, resulting in enhanced calpain activity, and this has been proposed as an important disease mechanism[4]. One possibility is that calpains enhance mutant huntingtin cleavage and processing[5–7]. However, the calpain cleavage sites are outside the exon 1 huntingtin fragment, so calpain cleavage of mutant huntingtin is not a factor influencing the aggregation and toxicity in such N-terminal fragment disease models (**Supplementary Fig. 1a**).

In addition to mutant huntingtin, autophagy also regulates the clearance of other aggregate-prone disease-causing proteins, such as those causing spinocerebellar ataxias types 1 and 3, forms of tau (causing fronto-temporal dementias) and the A53T and A30P α-synuclein mutants (which cause familial Parkinson's disease (PD))[8–15]. Autophagy induction reduces both soluble mutant huntingtin levels and inclusion frequencies, and attenuates its toxicity in cell, *Drosophila melanogaster* and mouse models of HD[8–12]. Autophagy induction may also be a valuable strategy in the treatment of infectious diseases, including tuberculosis, and may protect against cell death in certain contexts[16–18].

Currently, the only suitable pharmacological strategy for upregulating autophagy in mammalian brains is to use rapamycin (1), which inhibits mTOR (ref. 9). Also, since rapamycin is an immunosuppressant, it is contra-indicated for use in diseases like tuberculosis. The mechanism by which mTOR regulates autophagy remains unclear, and this kinase controls several cellular processes besides autophagy,

[1]Department of Medical Genetics, University of Cambridge, Cambridge Institute for Medical Research, Addenbrooke's Hospital, Hills Road, Cambridge CB2 0XY, UK. [2]Summit plc, 7340 Cambridge Research Park, Beach Drive, Waterbeach, Cambridge CB25 9TN, UK. [3]Department of Genetics, University of Cambridge, Downing Street, Cambridge CB2 3EH, UK. [4]Department of Neurology, Addenbrooke's Hospital, Hills Road, Cambridge CB2 2QQ, UK. [5]Department of Medicine, University of Cambridge, Cambridge Institute for Medical Research, Addenbrooke's Hospital, Hills Road, Cambridge CB2 0XY, UK. [6]These authors contributed equally to this work. Correspondence should be addressed to D.C.R. (dcr1000@hermes.cam.ac.uk).

Received 30 November 2007; accepted 7 February 2008; published online 23 March 2008; doi:10.1038/nchembio.79

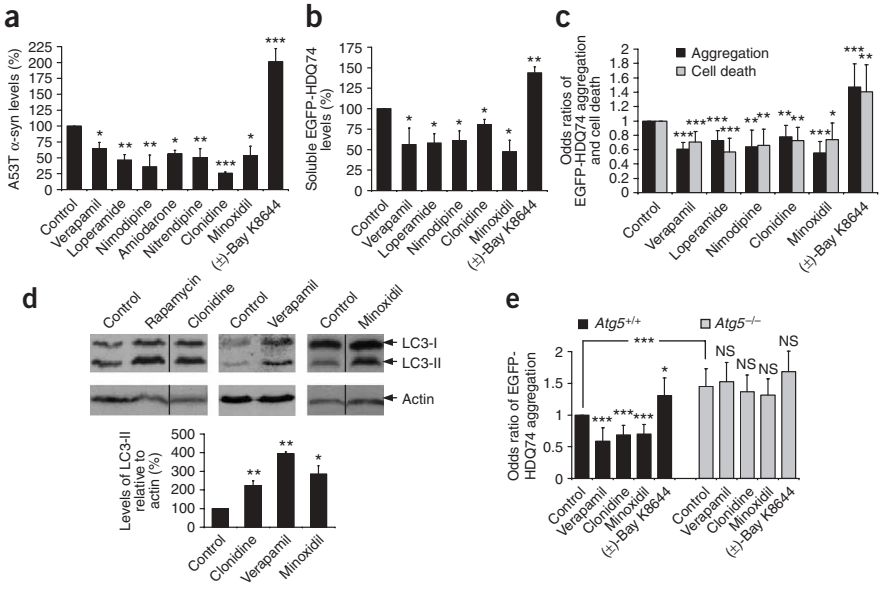

Figure 1 Identification of autophagy-inducing drugs. (**a**) Densitometric analysis relative to actin of A53T α-synuclein clearance in stable inducible PC12 cell line expressing A53T α-synuclein. Transgene expression was induced with doxycycline for 48 h, and then switched off (by removing doxycycline), with drug (all 1 μM) or DMSO (control) treatment for 24 h. Control condition is set to 100%. Error bars show s.e.m. (**b**) Densitometric analysis relative to actin of soluble EGFP-HDQ74 clearance in stable inducible PC12 cell line expressing EGFP-HDQ74. Transgene expression was induced with doxycycline for 8 h, and then switched off (by removing doxycycline) with drug (all 1 μM) or DMSO (control) treatment for 96 h. Control condition is set to 100%. Error bars show s.e.m. (**c**) SK-N-SH cells transfected with EGFP-HDQ74 construct for 4 h were treated with drugs (all 1 μM) or DMSO (control) for 48 h post-transfection. The proportions of EGFP-positive cells with aggregates or cell death were expressed as odds ratios and the control was taken as 1. Error bars show 95% confidence interval. (**d**) PC12 cells were treated with clonidine, minoxidil and verapamil (all 1 μM) or DMSO (control) for 24 h. Endogenous LC3-II levels were detected with anti-LC3 antibody and quantified relative to actin. Rapamycin (0.2 μM) was positive control. Error bars show s.e.m. (**e**) The proportions of EGFP-positive cells with EGFP-HDQ74 aggregates in wild-type (*Atg5*$^{+/+}$) and knockout (*Atg5*$^{-/-}$) Atg5 MEFs, transfected with EGFP-HDQ74 for 4 h and then treated for 48 h with drugs (all 1 μM) or DMSO (control). Error bars show 95% confidence interval. ***$P < 0.001$; **$P < 0.01$; *$P < 0.05$; NS, nonsignificant.

probably contributing to the complications seen with its long-term use[19]. Thus, we sought to identify new pathways and therapeutic agents that enhance autophagy. We found that L-type Ca^{2+} channel antagonists, a K^+_{ATP} channel opener and G_i signaling activators induce autophagy. These drugs revealed a cyclical mTOR-independent pathway regulating autophagy, in which cyclic AMP (**2**) regulates inositol 1,4,5-trisphosphate (IP_3, **3**) levels, influencing calpain activity, which completes the cycle by cleaving and activating $G_{s\alpha}$, which regulates cAMP levels. This pathway has numerous potential points where autophagy can be induced, and we provide proof of principle for therapeutic relevance in HD using cell, fly and zebrafish models.

RESULTS

Screen for autophagy enhancers

We screened for autophagy enhancers using a library of 253 compounds that includes drugs that had previously been used in humans without major toxic side effects, and pharmacological probes (see Methods). Our primary screen assayed clearance of A30P α-synuclein, a known autophagy substrate, in stable inducible PC12 cells[14,20]. All compounds that visibly altered A30P α-synuclein clearance were retested in multiple experiments in similar PC12 cell lines expressing A53T α-synuclein and were successfully validated. A53T α-synuclein clearance was enhanced by compounds including known autophagy inducers such as rapamycin and valproate[11,14] (**4**) (data not shown) and the following hits: five drugs that antagonize L-type Ca^{2+} channel activity (verapamil (**5**), loperamide (**6**), nimodipine (**7**), nitrendipine (**8**) and amiodarone (**9**)), minoxidil (**10**; an ATP-sensitive K^+ channel agonist) and clonidine (**11**; binds to α_2-adrenergic and type I imidazoline receptors and activates G_i protein signaling pathways) (**Fig. 1a** and **Supplementary Fig. 2a** online). (±)-Bay K8644 (**12**) (an L-type Ca^{2+} channel agonist[21]) retarded A53T α-synuclein clearance (**Fig. 1a** and **Supplementary Figs. 2a,b**). **Supplementary Figure 1b** summarizes characteristics of screen hits and other compounds used in the paper.

We prioritized our validation studies on minoxidil, clonidine and three L-type Ca^{2+} channel antagonists that act at different sites on these channels (verapamil, loperamide and nimodipine[22]). All of these compounds enhanced clearance of soluble mutant huntingtin exon 1 with 74Q (EGFP-HDQ74) in stable PC12 cells (which show no toxicity at these time points) and reduced its aggregation and toxicity in SK-N-SH (neuroblastoma) cells, whereas (±)-Bay K8644 had opposite effects (**Fig. 1b,c** and **Supplementary Fig. 2c**).

Clonidine, minoxidil and verapamil increase autophagy

We assessed autophagosome numbers using the microtubule-associated protein 1 light chain 3 (LC3)[23]. LC3 is processed post-translationally into LC3-I, then converted to LC3-II, the only known protein that specifically associates with autophagosome membranes[24]. LC3-positive vesicle numbers or LC3-II levels (versus actin) correlate with autophagosome numbers[23]. LC3-II levels were increased by clonidine, minoxidil and a representative Ca^{2+} channel antagonist, verapamil, which suggests enhanced autophagy (**Fig. 1d** and **Supplementary Fig. 2d**).

We confirmed that these drugs and (±)-Bay K8644 influence huntingtin aggregation in an autophagy-dependent manner, as they had no effects in autophagy-deficient mouse embryonic fibroblasts (MEFs) that have a knockout of the key autophagy gene *Atg5* (*Atg5*$^{-/-}$), whereas their effects in wild-type MEFs (*Atg5*$^{+/+}$) mirrored those in SK-N-SH cells (**Fig. 1e**).

Clonidine signals via the imidazoline type 1 receptor

Clonidine binds both α_2-adrenergic (α_2-AR) and imidazoline-1 (I1R) receptors. When clonidine binds α_2-AR, G_i signaling pathways are activated that reduce cAMP levels by inhibiting adenylyl cyclase[25]. I1R binding also reduces cAMP levels, although whether this is mediated by G proteins is disputed[26,27] (**Supplementary Fig. 3a** online). As clonidine had beneficial effects in both PC12 cells (which do not have α_2-AR but have I1R) and SK-N-SH cells (which have both these

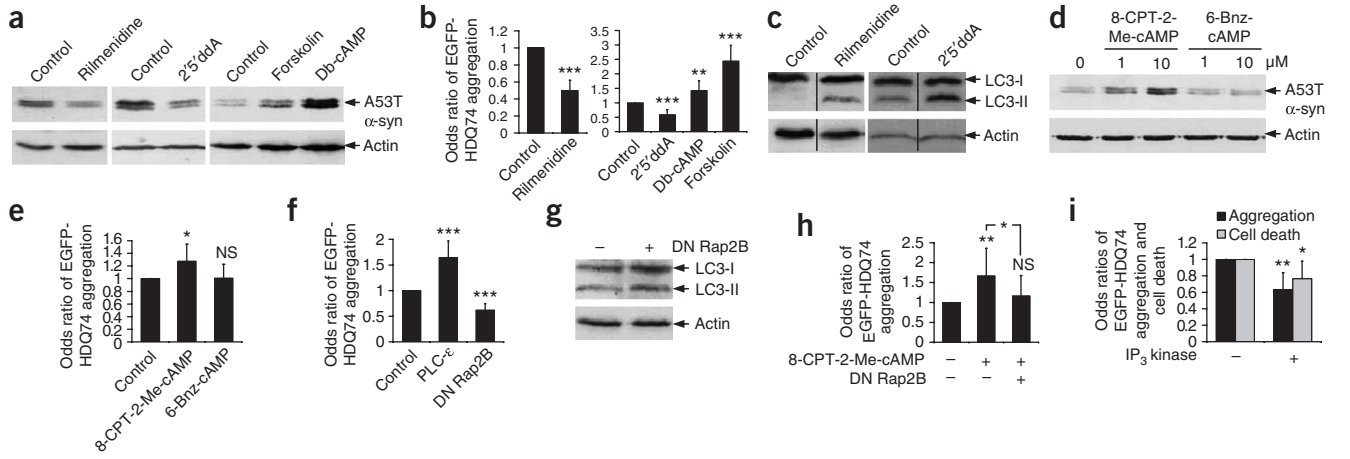

Figure 2 I1R agonists act through cAMP on Rap2B and PLC-ε to modulate autophagy. (**a**) A53T α-synuclein clearance in stable PC12 cells as in **Figure 1a**, treated with or without 1 μM rilmenidine, 1 mM dibutyl-cAMP (db-cAMP), 24 μM forskolin or 500 μM 2′5′-dideoxyadenosine (2′5′ddA) for 24 h. Note that control clearance levels for a given substrate may vary from figure to figure, due to different exposures of blots, which aid illustration of agents that either increase or retard clearance. (**b**) The proportions of EGFP-positive cells with EGFP-HDQ74 aggregates in SK-N-SH (for rilmenidine) and COS-7 (for db-cAMP, forskolin and 2′5′ddA) cells as in **Figure 1c**, treated with concentrations used in **a** for 48 h post-transfection. Error bars show 95% confidence interval. (**c**) Endogenous LC3-II levels in PC12 cells treated with 1 μM rilmenidine or 500 μM 2′5′ddA for 24 h. (**d**) A53T α-synuclein clearance in stable PC12 cells as in **Figure 1a**, treated with or without 8-CPT-2Me-cAMP or 6-Bnz-cAMP (1 μM or 10 μM). (**e**) The proportions of EGFP-positive COS-7 cells with aggregates as in **Figure 1c**, treated with or without 10 μM 8-CPT-2Me-cAMP or 6-Bnz-cAMP for 48 h post-transfection. Error bars show 95% confidence interval. (**f**) COS-7 cells, transfected for 4 h with EGFP-HDQ74 along with empty vector (pcDNA3.1), dominant-negative S17N Rap2B (DN Rap2B) or wild-type PLC-ε (1:3 ratio), were assessed for the proportions of EGFP-positive cells with aggregates after 48 h. Error bars show 95% confidence interval. (**g**) Endogenous LC3-II levels in COS-7 cells transfected with a dominant-negative Rap2B (DN Rap2B) for 4 h were assessed after 48 h expression. (**h**) The proportions of EGFP-positive COS-7 cells with aggregates, transfected with EGFP-HDQ74 along with empty vector (pcDNA3.1) or dominant-negative Rap2B (1:3 ratio) for 4 h, were treated with or without 10 μM 8-CPT-2Me-cAMP for 48 h. Error bars show 95% confidence interval. (**i**) COS-7 cells, transfected with EGFP-HDQ74 and dsRed2 or cytosolic dsRed2-IP_3 kinase A (1:3 ratio) for 4 h, were assessed at 48 h post-transfection for aggregation and cell death (as in **Fig. 1c**). Error bars show 95% confidence interval. $^{***}P < 0.001$; $^{**}P < 0.01$; $^{*}P < 0.05$; NS, nonsignificant.

receptors), we confirmed that rilmenidine (13) (a clinically approved centrally acting drug that binds I1R at ~30-fold higher affinity than the α_2-AR) could also enhance A53T α-synuclein clearance and decrease EGFP-HDQ74 aggregation in PC12 and SK-N-SH cells, respectively (**Fig. 2a**,**b** and **Supplementary Fig. 3b**). Rilmenidine, like clonidine and verapamil, also increased LC3-II levels in a dose-dependent manner (**Fig. 2c** and **Supplementary Figs. 2d** and **3c**).

I1R agonists signal via cAMP-Epac-Rap2B-PLC

Clonidine and rilmenidine likely act by reducing cAMP levels, as the adenylyl cyclase inhibitor 2′5′-dideoxyadenosine (2′5′ddA, 14) also enhanced A53T α-synuclein clearance and decreased EGFP-HDQ74 aggregation, whereas the cAMP analog dibutyryl cAMP (15) and the adenylyl cyclase activator forskolin (16) had opposite effects (**Fig. 2a**,**b** and **Supplementary Figs. 3a**,**b**). Furthermore, LC3-II levels were increased by 2′5′ddA (**Fig. 2c** and **Supplementary Fig. 3c**).

cAMP can signal to at least three different pathways: protein kinase A (PKA), Epac (a guanine nucleotide exchange factor) and through cyclic nucleotide-activated ion channels (**Supplementary Fig. 3a**)[28]. As the latter route does not operate at the cAMP levels expected by some of our treatments[28], we tested the former options. The Epac-specific cAMP analog 8-CPT-2-Me-cAMP (17) slowed A53T α-synuclein clearance and enhanced mutant huntingtin aggregation, whereas the PKA-specific cAMP analog 6-Bnz-cAMP (18) had no effect (**Fig. 2d**,**e** and **Supplementary Fig. 3d**). Likewise, KT 5720 (19), a PKA inhibitor, did not enhance A53T α-synuclein clearance—it had the reverse effect (**Supplementary Fig. 3e**). Henceforth, we focused on the Epac pathway and tested its downstream components.

Epac activates the small GTPase Rap2B, which in turn activates the ubiquitously expressed phospholipase C (PLC)-ε isoform[29], which hydrolyzes phosphatidylinositol 4,5-bisphosphate (PIP_2, 20) to form IP_3 and diacylglycerol (DAG, 21) (**Supplementary Fig. 3a**). This pathway is well conserved in many cell types including neurons, neuronal cells like PC12 cells, and COS-7 cells[30–33]. We have confirmed Rap2B activation in PC12 cells treated with forskolin (**Supplementary Fig. 3f**). This established pathway from G_i-coupled receptors to PLC-ε was a strong candidate autophagy regulator, as IP_3 negatively regulates autophagy in an mTOR-independent fashion, and a recent study has shown induction of autophagy after IP_3 receptor (IP_3R) knockdown[11,34,35]. Consistent with this hypothesis, dominant-negative S17N Rap2B decreased EGFP-HDQ74 aggregation, while overexpression of PLC-ε enhanced EGFP-HDQ74 aggregation (**Fig. 2f**). The protective effects of dominant-negative Rap2B on EGFP-HDQ74 aggregation were associated with an increase in LC3-II levels (**Fig. 2g** and **Supplementary Fig. 3g**). Consistent with a link between Epac and Rap2B, the deleterious effects of the Epac-specific cAMP analog 8-CPT-2-Me-cAMP on huntingtin aggregation were abrogated by dominant-negative Rap2B (**Fig. 2h** and **Supplementary Fig. 3h**). Furthermore, overexpression of cytosolic IP_3 kinase A (ref. 36)—which catalyzes the phosphorylation of IP_3, generating inositol 1,3,4,5-tetrakisphosphate (IP_4, 22), thereby inactivating the signal for endoplasmic reticulum Ca^{2+} release—decreased EGFP-HDQ74 aggregation and toxicity (**Fig. 2i**).

PLC/IP_3 and L-type Ca^{2+} channels regulate calpain activity

The pathway from cAMP to IP_3 regulates intracytosolic Ca^{2+} levels, as IP_3 binds to endoplasmic reticulum receptors, thereby facilitating Ca^{2+}

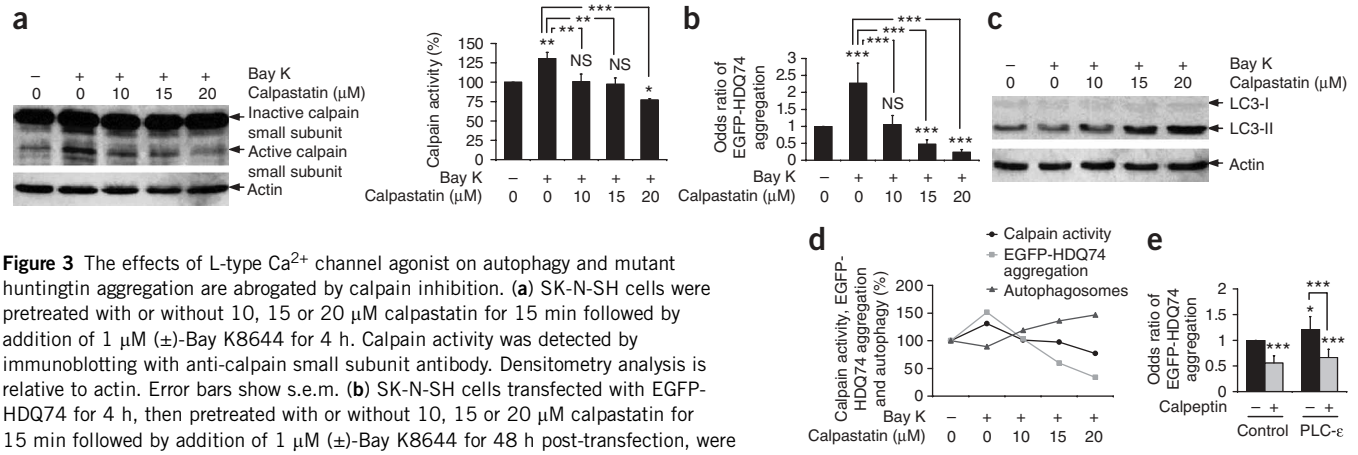

Figure 3 The effects of L-type Ca^{2+} channel agonist on autophagy and mutant huntingtin aggregation are abrogated by calpain inhibition. (**a**) SK-N-SH cells were pretreated with or without 10, 15 or 20 μM calpastatin for 15 min followed by addition of 1 μM (±)-Bay K8644 for 4 h. Calpain activity was detected by immunoblotting with anti-calpain small subunit antibody. Densitometry analysis is relative to actin. Error bars show s.e.m. (**b**) SK-N-SH cells transfected with EGFP-HDQ74 for 4 h, then pretreated with or without 10, 15 or 20 μM calpastatin for 15 min followed by addition of 1 μM (±)-Bay K8644 for 48 h post-transfection, were assessed for the proportion of EGFP-positive cells with EGFP-HDQ74 aggregates. Error bars show 95% confidence interval. (**c**) SK-N-SH cells were pretreated with or without 10, 15 or 20 μM calpastatin for 15 min followed by addition of 1 μM (±)-Bay K8644 for 4 h. Endogenous LC3-II levels were detected by immunoblotting with anti-LC3 antibody. (**d**) Comparison between calpain activity, EGFP-HDQ74 aggregation and autophagosomes as seen in **a–c**. The control condition for all the assessments was set at 100%. Calpastatin lowered the increased calpain activity and EGFP-HDQ74 aggregation caused by (±)-Bay K8644 in a dose-dependent manner with a simultaneous increase in LC3-II levels (autophagosomes). (**e**) COS-7 cells transfected with empty vector (pcDNA3.1) or wild-type PLC-ε for 4 h and treated with or without 50 μM calpeptin for 48 h post-transfection were assessed for the proportion of EGFP-positive cells with EGFP-HDQ74 aggregates. Error bars show 95% confidence interval. $^{***}P < 0.001$; $^{**}P < 0.01$; $^{*}P < 0.05$; NS, nonsignificant.

release from this organelle. Likewise, L-type Ca^{2+} channel antagonists are known to decrease intracytosolic Ca^{2+}, and L-type Ca^{2+} channel agonists increase intracytosolic Ca^{2+} concentrations (**Supplementary Fig. 3a,i**). Intracytosolic Ca^{2+} activates calpains[37]. The two ubiquitously expressed mammalian calpains, calpain 1 (μ-calpain) and calpain 2 (m-calpain), are heterodimeric proteins comprising a distinct 80-kDa large catalytic subunit and a common 28-kDa small regulatory subunit, which is converted from the 28-kDa (inactive) form to a 21-kDa polypeptide (active) following activation by increased cytosolic Ca^{2+} (for example, with thapsigargin (23) (**Supplementary Fig. 3j**))[37]. PLC-ε overexpression, and treatments with (±)-Bay K8644 and 8-CPT-2-Me-cAMP, also increased calpain activity (**Fig. 3a** and **Supplementary Fig. 3k,l**).

Calpain activity is enhanced in HD *in vivo*[4], and we confirmed that this elevation could be normalized by calpastatin or verapamil in our stable inducible cell models (**Supplementary Fig. 3m**). Very low calpain activity in the basal state makes reliable assessment of inhibitory effects even of specific calpain inhibitors difficult in whole cells with normal intracellular Ca^{2+} concentrations.

Minoxidil decreases whole-cell L-type Ca^{2+} channel currents in a concentration-dependent manner[38]. In contrast to minoxidil, K^{+}_{ATP} channel blockers, such as quinine sulfate (24) and tolazamide (25), slow clearance of autophagy substrates (**Supplementary Fig. 2e,f**). Because minoxidil is likely to act via the same pathway as the L-type Ca^{2+} channel blockers, we have restricted further pathway analyses to the Ca^{2+} channel blockers.

Calpain inhibition reduces mutant huntingtin aggregation

We tested calpains as central to autophagy regulation as they are common targets of the two major pathways identified by our screen hits—the cAMP-Epac-PLC-IP_3 (clonidine) and the L-type Ca^{2+} channel pathways. This possibility was consistent with the calpain inhibitor calpastatin inhibiting the levels of calpain activation mediated by (±)-Bay K8644 in a dose-dependent manner (**Fig. 3a**). Both calpastatin and verapamil (which also abrogates calpain activation) rescued the effects of (±)-Bay K8644 on EGFP-HDQ74 aggregation (**Fig. 3b** and **Supplementary Fig. 3n,o**). Likewise, calpastatin enhanced LC3-II levels in the presence of (±)-Bay K8644 in a manner that correlated with the decrease in EGFP-HDQ74 aggregation and calpain activity (**Fig. 3c,d**). Furthermore, calpeptin (26), another calpain inhibitor, rescued the increased EGFP-HDQ74 aggregation induced by overexpression of PLC-ε (**Fig. 3e**).

It is important to point out that 10 μM calpastatin reduced calpain activation and EGFP-HDQ74 aggregation, and increased autophagic activity to around baseline levels (as in DMSO-treated control condition) in (±)-Bay K8644–treated cells (**Fig. 3a–d**). However, 20 μM calpastatin resulted in lower calpain activity and EGFP-HDQ74 aggregation, and simultaneously increased autophagy in (±)-Bay K8644–treated cells, even compared to DMSO-treated (control) cells (**Fig. 3a–d**). Thus, this places calpain downstream of L-type Ca^{2+} channels in this pathway (**Supplementary Fig. 3a**).

We confirmed the predictions from the above data that calpain inhibitors and small interfering RNA knockdown of either calpain 1 or calpain 2 would reduce EGFP-HDQ74 aggregation and toxicity in cells not exposed to other drugs (**Fig. 4a–c**). Calpain inhibition enhanced the clearance of EGFP-HDQ74 and A53T α-synuclein (in undifferentiated and differentiated neuronal PC12 cells) (**Fig. 4d,e**).

Conversely, overexpression of constitutively active S50E human m-calpain increased EGFP-HDQ74 aggregation and toxicity (**Fig. 4f**). The effects of constitutively active m-calpain on EGFP-HDQ74 aggregation were not abrogated by either verapamil or clonidine (**Fig. 4g**), again consistent with calpain being downstream of the L-type Ca^{2+} channel (verapamil) and the cAMP-Epac-PLC-IP_3 (clonidine) pathways.

Consistent with these data, thapsigargin increased EGFP-HDQ74 aggregates and toxicity and delayed A53T α-synuclein clearance—effects that were attenuated by calpain inhibitors (**Supplementary Fig. 4a–j** online).

Calpain inhibition induces autophagy

We next tested whether the reduced EGFP-HDQ74 aggregation mediated by the calpain inhibitors was autophagy dependent.

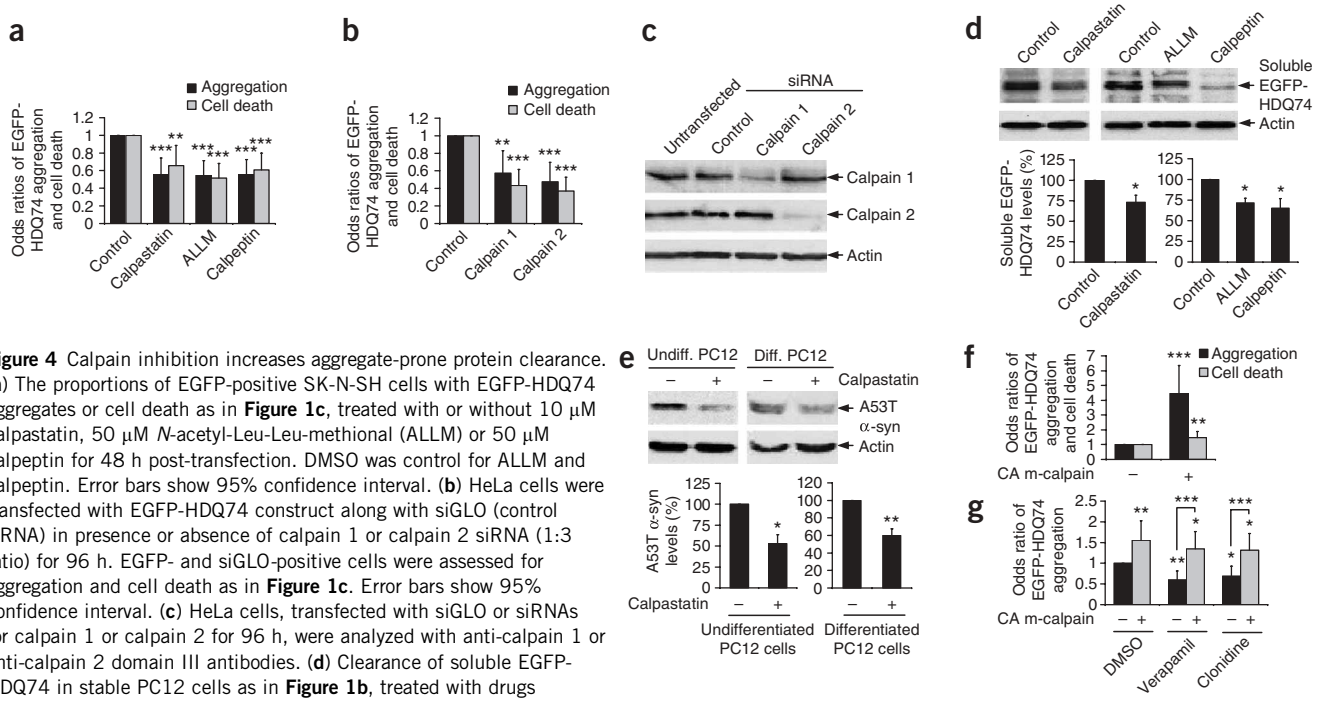

Figure 4 Calpain inhibition increases aggregate-prone protein clearance. (**a**) The proportions of EGFP-positive SK-N-SH cells with EGFP-HDQ74 aggregates or cell death as in **Figure 1c**, treated with or without 10 μM calpastatin, 50 μM *N*-acetyl-Leu-Leu-methional (ALLM) or 50 μM calpeptin for 48 h post-transfection. DMSO was control for ALLM and calpeptin. Error bars show 95% confidence interval. (**b**) HeLa cells were transfected with EGFP-HDQ74 construct along with siGLO (control siRNA) in presence or absence of calpain 1 or calpain 2 siRNA (1:3 ratio) for 96 h. EGFP- and siGLO-positive cells were assessed for aggregation and cell death as in **Figure 1c**. Error bars show 95% confidence interval. (**c**) HeLa cells, transfected with siGLO or siRNAs for calpain 1 or calpain 2 for 96 h, were analyzed with anti-calpain 1 or anti-calpain 2 domain III antibodies. (**d**) Clearance of soluble EGFP-HDQ74 in stable PC12 cells as in **Figure 1b**, treated with drugs (concentrations in **a**) for 96 h. Densitometry is relative to actin. Error bars show s.e.m. (**e**) A53T α-synuclein clearance in undifferentiated or nonmitotic neuronally differentiated (with 100 ng ml^{-1} nerve growth factor for 5 d) stable PC12 cells as in **Figure 1a**, treated with or without 10 μM calpastatin for 24 h. Densitometry is relative to actin. Error bars show s.e.m. (**f**) COS-7 cells, transfected with EGFP-HDQ74 along with empty vector (pcDNA3.1) or constitutive active (CA) m-calpain (1:3 ratio) for 48 h, were assessed for aggregation and cell death as in **Figure 1c**. Error bars show 95% confidence interval. (**g**) SK-N-SH cells, transfected with EGFP-HDQ74 along with empty vector (pcDNA3.1) or constitutive active m-calpain (1:3 ratio) for 4 h, were subsequently treated with DMSO (control), 1 μM verapamil or 1 μM clonidine for 48 h. The proportions of EGFP-positive cells with aggregates were assessed as in **Figure 1c**. Error bars show 95% confidence interval. $^{***}P < 0.001$; $^{**}P < 0.01$; $^{*}P < 0.05$.

Calpastatin could not reduce EGFP-HDQ74 aggregates in *Atg5*$^{-/-}$, but reduced aggregates in *Atg5*$^{+/+}$ MEFs, or when wild-type (but not conjugation-deficient) Atg5 (K130R) was overexpressed in *Atg5*$^{-/-}$ cells (**Fig. 5a**).

Calpain 1 or calpain 2 knockdown by siRNA and calpain inhibitors increased LC3 vesicle and autophagosome numbers (**Fig. 5b** and **Supplementary Fig. 5a–c** online). Calpeptin also increased the number of autophagosome-like structures and decreased the numbers of mitochondria (which are endogenous autophagy substrates[2]) in COS-7 cells as evaluated by electron microscopy (**Supplementary Fig. 5d,e**). Consistent with the data in **Supplementary Figure 4f–j**, thapsigargin-treated cells pretreated with calpain inhibitors had more autophagosomes than cells treated with thapsigargin only (**Supplementary Fig. 4k,l**).

LC3-II levels also accumulated in cells treated with calpastatin (**Fig. 5c** and **Supplementary Fig. 5f**). LC3-II accumulation can occur due to increased autophagosome formation or impaired autophagosome-lysosome fusion. Thus, we assayed LC3-II in the presence of bafilomycin A1 (27), which blocks autophagosome-lysosome fusion, to assess autophagosome formation[39]. Bafilomycin A1 increases LC3-II (**Fig. 5d** and **Supplementary Fig. 5g**), and the concentration used is saturating for LC3-II levels in this assay (data not shown). Further blockage of autophagosome-lysosome fusion via a bafilomycin A1–independent mechanism, using the dynein inhibitor erythro-9-(3-(2-hydroxynonyl)) adenine (EHNA)[40] (28), along with this dose of bafilomycin A1, results in no increase in LC3-II compared to bafilomycin A1 alone (data not shown). We have previously demonstrated that autophagy inducers can further increase LC3-II levels in bafilomycin A1–treated cells, which indicates that such compounds increase autophagosome formation[10,12]. To test whether calpain inhibitors induce autophagosome formation, we pretreated EGFP-LC3 HeLa cells with the inhibitors for 24 h and then added bafilomycin A1 to the cells for a further 4 h. We assumed that calpain inhibitors act by blocking clearance or cleavage of key autophagy regulators, and thus some time is needed for these putative regulators to accumulate. Calpain inhibitors increased LC3-II levels in the presence of bafilomycin A1, compared to bafilomycin A1 alone, which suggests induction of autophagy (**Fig. 5d** and **Supplementary Fig. 5g**). Likewise, L-type Ca^{2+} channel antagonist (verapamil) showed a similar trend (**Supplementary Fig. 5h**). Conversely, overexpression of constitutively active m-calpain reduced Myc-LC3-II levels and EGFP-LC3 vesicle numbers (**Fig. 5e,f**).

Though our data suggest that thapsigargin inhibits clearance of various autophagy-dependent substrates by activating calpains (**Supplementary Fig. 4a–j**), it appears to have additional effects on autophagy. In contrast to overexpression of m-calpain, which reduces autophagosome numbers (**Fig. 5e,f**), thapsigargin increased steady state levels of LC3 vesicles and LC3-II (**Supplementary Fig. 4m,n**). However, thapsigargin did not increase LC3-II levels in bafilomycin A1–treated cells, compared to the levels with bafilomycin A1 alone (**Supplementary Fig. 4n**), which was in contrast to the effects of various autophagy inducers[10,12] (**Fig. 5d** and **Supplementary Fig. 5g,h**). The phenomenon of an agent that decreases clearance of autophagy substrates, and that also increases steady state autophagosome numbers but does not increase autophagosome levels in cells treated with bafilomycin A1, is characteristic of compounds and genes

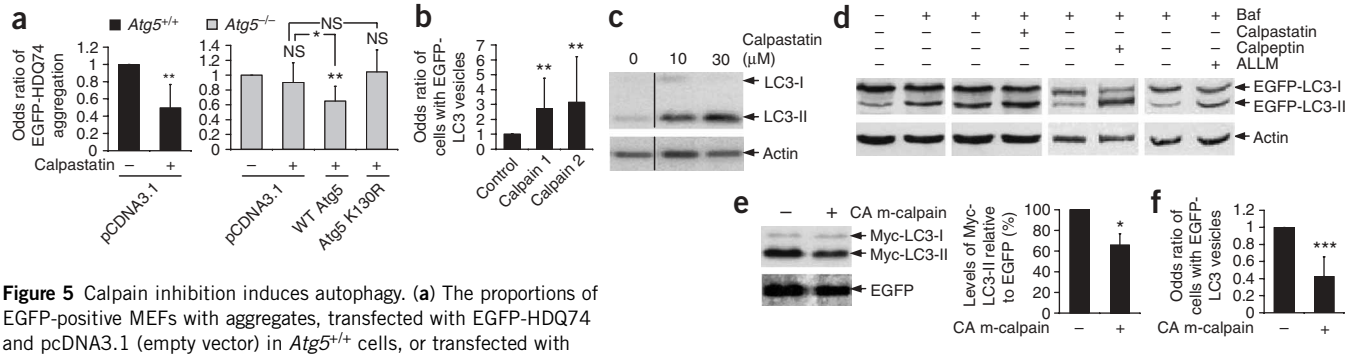

Figure 5 Calpain inhibition induces autophagy. (**a**) The proportions of EGFP-positive MEFs with aggregates, transfected with EGFP-HDQ74 and pcDNA3.1 (empty vector) in *Atg5*$^{+/+}$ cells, or transfected with EGFP-HDQ74 and pcDNA3.1, WT Atg5 or K130R Atg5 constructs in *Atg5*$^{-/-}$ cells for 4 h (1:3 ratios), were treated for next 48 h with or without 10 μM calpastatin. All data are from the same experiment, but odds ratios for reference conditions in specific experiments have been set to 1, to facilitate comparisons. *Atg5*$^{-/-}$ cells had increased EGFP-HDQ74 aggregates compared to *Atg5*$^{+/+}$ cells[10,12]. Error bars show 95% confidence interval. (**b**) HeLa cells were transfected with siGLO (control) with or without calpain 1 siRNA or calpain 2 siRNA (1:3 ratio) for 96 h, followed by transfection with EGFP-LC3 construct for 4 h. Cells were fixed after a further 2 h. The proportions of transfected cells with >5 EGFP-LC3 vesicles were assessed. Error bars show 95% confidence interval. (**c**) Endogenous LC3-II levels in SK-N-SH cells treated with or without 10 μM or 30 μM calpastatin for 24 h. (**d**) HeLa cells stably expressing EGFP-LC3 were treated for 4 h with 400 nM bafilomycin A1 in presence or absence of 10 μM calpastatin, 50 μM ALLM or 50 μM calpeptin. Calpain inhibitors were treated for 24 h before bafilomycin A1 addition. EGFP-LC3-II was detected with anti-EGFP antibody. Data from different calpain inhibitors are from different blots. (**e**) COS-7 cells, transfected with myc-LC3 and EGFP-C1 with pcDNA3.1 (empty vector) or constitutively active (CA) m-calpain (1:1:3 ratio) for 4 h, were analyzed after 24 h post-transfection for LC3-II levels by immunoblotting with anti-myc antibody. Error bars show s.e.m. (**f**) COS-7 cells, transfected with EGFP-LC3 and pcDNA3.1 (empty vector) or CA m-calpain (1:3 ratio) for 4 h and fixed 24 h post-transfection, were assessed for proportions of EGFP-positive cells with >5 EGFP-LC3 vesicles. Error bars show 95% confidence interval. ***$P < 0.001$; **$P < 0.01$; *$P < 0.05$; NS, nonsignificant.

that block autophagosome-lysosome fusion[10,40]. Such agents and genes also result in lower proportions of LC3 vesicles colocalizing with the lysosomal marker lgp120 (Lamp1), which we observed with thapsigargin (**Supplementary Fig. 4o**)[10,12]. Thus, the most parsimonious explanation for our data is that thapsigargin decreases the clearance of autophagic substrates (**Supplementary Fig. 4a–d**) via at least two mechanisms: a calpain-dependent process that reduces autophagosome synthesis (**Fig. 5e,f** and **Supplementary Fig. 4f–l**) and a calpain-independent process that probably decreases autophagosome lysosome fusion (**Supplementary Fig. 4m–o**).

Autophagy induction by calpain inhibitors is not predominantly mediated by effects on Ca^{2+} levels in intracellular stores (such as the endoplasmic reticulum)[41]. Though the autophagy-inhibitory effect of thapsigargin was rescued by calpain inhibitors, there were no

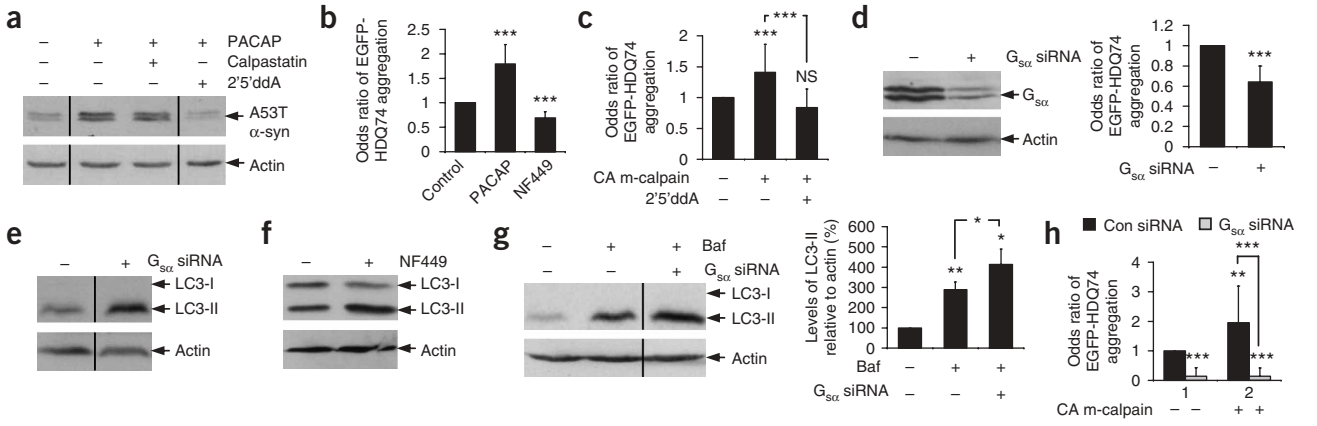

Figure 6 Calpain cleaves $G_{s\alpha}$, creating a link between the cAMP and Ca^{2+}-calpain pathways. (**a**) A53T α-synuclein clearance in stable PC12 cells as in **Figure 1a**, treated with or without 100 nM PACAP, with or without 10 μM calpastatin or 500 μM 2′5′ddA for 24 h. (**b**) The proportion of EGFP-positive cells with aggregates in SK-N-SH cells as in **Figure 1c**, treated for 48 h with 1 μM PACAP or 200 μM NF449. Error bars show 95% confidence interval. (**c**) Aggregation in COS-7 cells transfected with either pcDNA3:1 (empty vector) or constitutively active (CA) m-calpain and EGFP-HDQ74 (3:1 ratio) for 4 h and then treated with or without 500 μM 2′5′ddA for 48 h. Error bars show 95% confidence interval. (**d**) HeLa cells transfected with control or $G_{s\alpha}$ siRNA for 72 h were analyzed for $G_{s\alpha}$ levels by immunoblotting with anti-$G_{s\alpha}$ antibody. Aggregation was assessed in HeLa cells transfected with control or $G_{s\alpha}$ siRNA and EGFP-HDQ74 for 72 h. Error bars show 95% confidence interval. (**e**) Endogenous LC3-II levels in HeLa cells transfected with control or $G_{s\alpha}$ siRNA for 72 h. (**f**) Endogenous LC3-II levels in PC12 cells treated with or without 200 μM NF449 for 24 h. (**g**) Endogenous LC3-II levels in HeLa cells transfected with control or $G_{s\alpha}$ siRNA for 72 h and treated with or without 400 nM bafilomycin A1 for the last 4 h. Densitometric analysis is relative to actin. Error bars show s.e.m. (**h**) The proportions of EGFP-positive HeLa cells with aggregates, transfected with control or $G_{s\alpha}$ siRNA for 48 h, and then retransfected together with pcDNA 3.1 (empty vector) or CA m-calpain and EGFP-HDQ74 (3:1 ratio) for a further 48 h. Error bars show 95% confidence interval. ***$P < 0.001$; **$P < 0.01$; *$P < 0.05$; NS, nonsignificant.

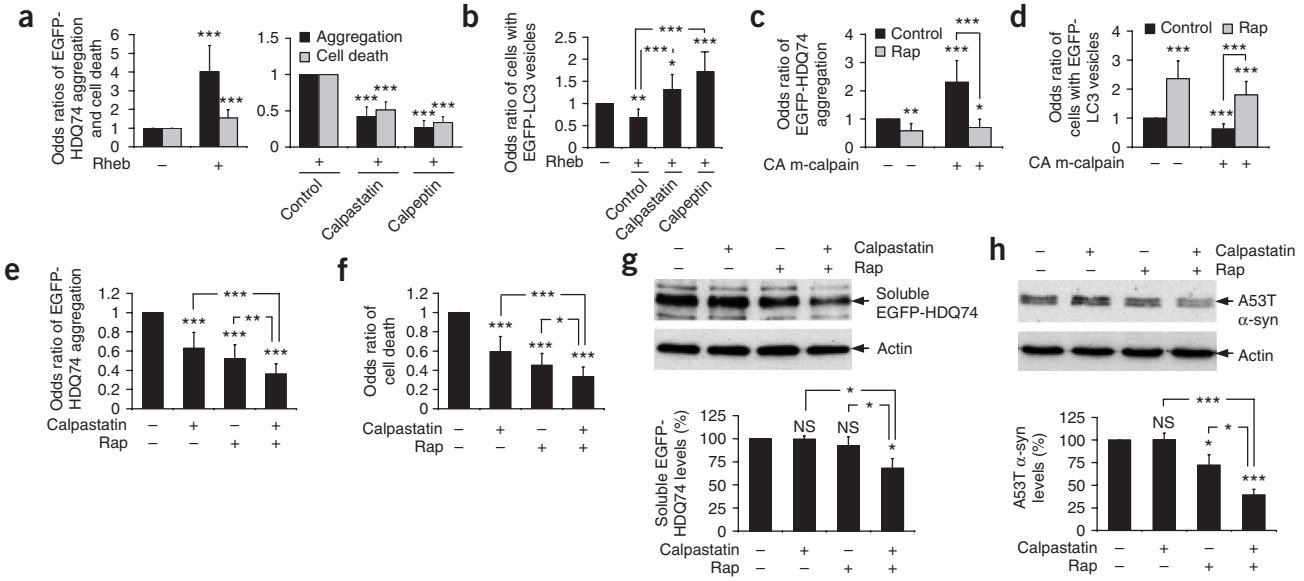

Figure 7 Regulation of autophagy by calpain is mTOR independent. (**a**) The proportions of EGFP-positive COS-7 cells with aggregates or cell death, after transfection with EGFP-HDQ74 and rheb or pcDNA3.1 (empty vector) (1:3 ratio) for 4 h and treatment with or without 10 μM calpastatin or 50 μM calpeptin for 48 h post-transfection. The control condition for assessing the effect of calpain inhibitors in rheb-transfected cells was taken as 1. Error bars show 95% confidence interval. (**b**) The proportions of EGFP-positive COS-7 cells with >5 EGFP-LC3 vesicles, transfected with EGFP-LC3 and pcDNA3.1 (empty vector) or rheb (1:3 ratio) for 4 h and treated with or without 10 μM calpastatin or 50 μM calpeptin for 24 h post-transfection. Error bars show 95% confidence interval. (**c**) The proportions of EGFP-positive COS-7 cells with aggregates, transfected with EGFP-HDQ74 and constitutively active (CA) m-calpain or pcDNA3.1 (empty vector) (1:3 ratio) for 4 h and treated with or without 0.2 μM rapamycin for 48 h post-transfection. Error bars show 95% confidence interval. (**d**) The proportions of EGFP-positive COS-7 cells with >5 EGFP-LC3 vesicles, transfected with EGFP-LC3 and CA m-calpain or pcDNA3.1 (empty vector) (1:3 ratio) for 4 h and treated with or without 0.2 μM rapamycin for 24 h post-transfection. Error bars show 95% confidence interval. (**e**,**f**) The proportions of EGFP-positive COS-7 cells with aggregates (**e**) and cell death (**f**) as in **Figure 1c**, treated with or without 0.2 μM rapamycin, 10 μM calpastatin or both for 48 h. Error bars show 95% confidence interval. (**g**) Clearance of soluble EGFP-HDQ74 in stable PC12 cells as in **Figure 1b**, treated with or without 0.2 μM rapamycin, 10 μM calpastatin or both for the 48 h switch-off period. Error bars show s.e.m. (**h**) Clearance of A53T α-synuclein in stable PC12 cells as in **Figure 1a**, treated with or without 0.2 μM rapamycin, 10 μM calpastatin or both for the 8 h switch-off period. Error bars show s.e.m. $***P < 0.001$; $**P < 0.01$; $*P < 0.05$; NS, nonsignificant.

significant differences in the stored Ca^{2+} between thapsigargin-treated cells with or without calpain inhibitors (**Supplementary Fig. 4p,q**).

$G_{s\alpha}$ is a calpain substrate regulating autophagy

In order to select candidate calpain substrates regulating autophagy, we considered which substrates would inhibit autophagy if subjected to low levels of cleavage. An appealing candidate was the α subunit of heterotrimeric G proteins ($G_{s\alpha}$), which increases its activity after calpain cleavage[42], because $G_{s\alpha}$ enhances adenylyl cyclase activity. We confirmed that the hallmark 20-kDa $G_{s\alpha}$ cleavage product appeared in our cells overexpressing constitutive active m-calpain, or in cells treated with thapsigargin (**Supplementary Fig. 6a** online).

Compatible with our hypothesis, activation of $G_{s\alpha}$ with its natural ligand, pituitary adenylyl cyclase–activating polypeptide (PACAP), increased cAMP levels and retarded A53T α-synuclein clearance (**Fig. 6a** and **Supplementary Fig. 6b–d**). This effect was not blocked by calpastatin (as PACAP activation can occur without $G_{s\alpha}$ cleavage) but was abolished by inhibition of its downstream target, adenyl cyclase (with 2′5′ddA) (**Fig. 6a** and **Supplementary Fig. 6c**). PACAP also enhanced EGFP-HDQ74 aggregation (**Fig. 6b**). Consistent with the hypothesis that calpains activate $G_{s\alpha}$, which mediates effects by enhancing adenylyl cyclase activity (confirmed in **Supplementary Fig. 6d,e**, where constitutively active m-calpain increased cAMP levels), 2′5′ddA decreased the enhanced EGFP-HDQ74 aggregation caused by overexpression of constitutively active m-calpain (**Fig. 6c**), in a manner similar to what we observed with PACAP (**Fig. 6a**).

Knockdown of $G_{s\alpha}$ with siRNA or treatment with its chemical inhibitor NF449 (29) decreased EGFP-HDQ74 aggregation and increased LC3-II levels (**Fig. 6b,d–f** and **Supplementary Fig. 6f**). The increase in LC3-II levels with $G_{s\alpha}$ knockdown by siRNA was also seen in cells treated with bafilomycin A1, which suggests that knockdown of $G_{s\alpha}$ increases autophagosome synthesis (**Fig. 6g**). $G_{s\alpha}$ is likely to mediate many of the autophagy-related effects of calpains on EGFP-HDQ74 aggregation, as the increased aggregation mediated by overexpression of constitutively active m-calpain was abrogated by $G_{s\alpha}$ siRNA, and the beneficial effects of calpain inhibition were not further enhanced in calpastatin-treated cells with $G_{s\alpha}$ knockdown (**Fig. 6h** and **Supplementary Fig. 6g**).

Another candidate we considered was Atg5, which may be cleaved by calpains in certain cell death contexts[43]. However, we observed no reduction in full-length Atg5, no obvious cleavage products in cells treated with thapsigargin and no increase in Atg5 levels with calpastatin (**Supplementary Fig. 6h**).

Calpain-regulated autophagy is mTOR independent

Calpain-regulated autophagy appeared to be independent of, or downstream of, the known pathway that is negatively regulated by mTOR, as its kinase activity, inferred by the levels of phosphorylation of its substrates (ribosomal S6 protein kinase (S6K1, also known as p70S6K) and eukaryotic initiation factor 4E-binding protein 1 (4E-BP1)[19]), was not reduced by calpain inhibitors (**Supplementary Fig. 6i,j**). Likewise, drugs that perturb

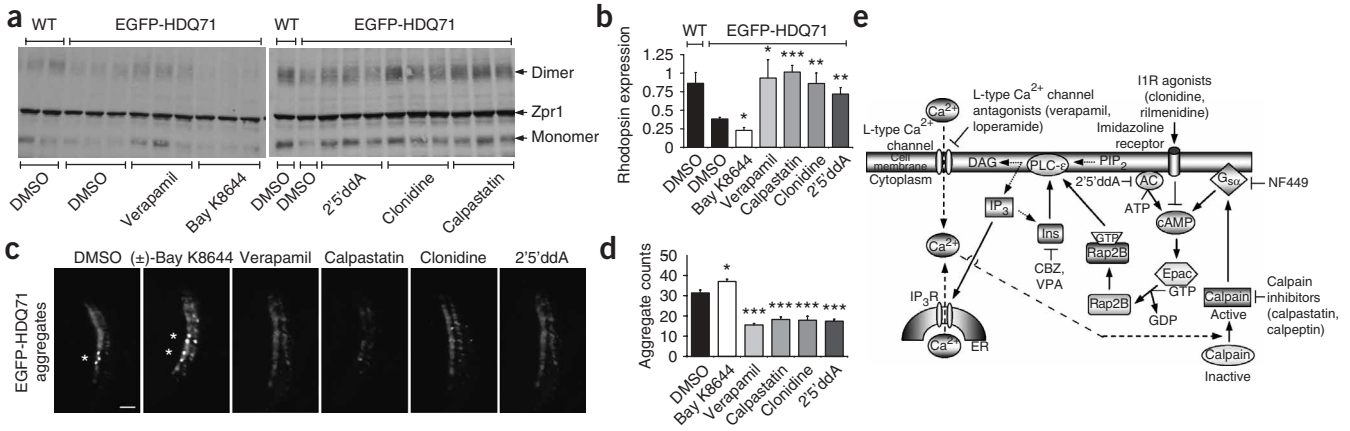

Figure 8 L-type Ca^{2+} channel antagonists, I1R agonists, cAMP antagonists and calpain inhibitors rescue Huntington's disease phenotypes in zebrafish. (**a**) Western blot showing EGFP-HDQ71–induced degeneration of rod photoreceptors at 9 d.p.f. as indicated by the decrease in the abundance of of monomeric (~36 kDa) and dimeric (~72 kDa) rhodopsin. Rhodopsin expression is further reduced by 3 μM (±)-Bay K8644, and recovered upon treatment with 3 μM verapamil, 100 μM 2′5′ddA, 3 μM clonidine and 1 μM calpastatin. No general toxicity to the zebrafish at these concentrations was observed. (**b**) Expression of EGFP-HDQ71 significantly reduces the levels of rhodopsin expression when compared to wild-type (WT) nontransgenic controls. This effect is further abrogated by 3 μM (±)-Bay K8644, whereas 3 μM verapamil, 100 μM 2′5′ddA, 3 μM clonidine and 1 μM calpastatin all protected against rod photoreceptor degeneration. Error bars show s.e.m. (**c**) Magnified bright field and EGFP images of zebrafish eye sections, taken at the ventral marginal zone for each of the indicated treatments (with concentrations as in **b**), are shown. Scale bar, 10 μm. $***P < 0.001$; $**P < 0.01$; $*P < 0.05$. (**d**) The total number of aggregates across 8 × 12 μm sections was counted and compared to the EGFP-HDQ71 DMSO-treated control. 3 μM (±)-Bay K8644 was found to significantly increase the aggregate burden, whereas 3 μM verapamil, 1 μM calpastatin, 3 μM clonidine and 100 μM 2′5′ddA decreased the aggregate load. As in our cell models, these aggregates were insoluble in 4% triton/SDS. Error bars show s.e.m. $***P < 0.001$; $**P < 0.01$; $*P < 0.05$. (**e**) Schematic representation of an mTOR-independent autophagy pathway involving cAMP-Ca^{2+}-calpains-$G_{s\alpha}$ with multiple drug targets. Intracellular cAMP levels are increased by adenylyl cyclase (AC) activity, thereby activating Epac, which subsequently activates Rap2B, a small G protein that activates PLC-ε, resulting in the production of IP_3 and consequent Ca^{2+} release from the endoplasmic reticulum (ER). Intracellular Ca^{2+} levels are also increased by L-type Ca^{2+} channel agonists. An increase in intracytosolic Ca^{2+} activates calpains, which cleave and activate $G_{s\alpha}$, which activates AC to increase cAMP levels, thereby forming a loop. Activation of this pathway inhibits autophagy. Multiple drug targets acting at various places in this pathway induce autophagy, including the following: I1R agonists (clonidine and rilmenidine) and the AC inhibitor 2′5′ddA, which decrease cAMP levels, agents lowering inositol and IP_3 levels (carbamazepine (CBZ) and valproic acid (VPA))[11], L-type Ca^{2+} channel antagonists (verapamil and loperamide), calpain inhibitors (calpastatin and calpeptin) and the $G_{s\alpha}$ inhibitor NF449.

intracellular Ca^{2+} such as thapsigargin had no effect on mTOR signaling (**Supplementary Fig. 4r**).

Overexpression of the small G protein rheb, which greatly enhances mTOR signaling, markedly increased EGFP-HDQ74 aggregates and cell death in COS-7 cells[9] (**Fig. 7a**). However, the calpain inhibitors reduced EGFP-HDQ74 aggregation and toxicity and increased EGFP-LC3 vesicle numbers in rheb-transfected cells (**Fig. 7a,b**), which suggests that induction of autophagy by calpain inhibition occurs even when mTOR is activated. Thus, calpain inhibitors do not act upstream of mTOR.

We next tested whether mTOR inhibition induced autophagy when calpains were activated. This is relevant to HD where calpains are activated, and where rapamycin is protective in *in vivo* models[4,5,8,9]. In cells overexpressing constitutively active m-calpain, rapamycin reduced EGFP-HDQ74 aggregation and increased autophagosome numbers, which further suggests that mTOR and calpains regulate autophagy via independent pathways (**Fig. 7c,d**). Similarly, rapamycin reduced the increased EGFP-HDQ74 aggregation and toxicity induced by thapsigargin, and increased EGFP-LC3 vesicle numbers in thapsigargin-treated cells (**Supplementary Fig. 4s–u**).

Simultaneous inhibition of calpain and mTOR

As calpain inhibition induces autophagy independently of mTOR, we confirmed that calpastatin and rapamycin have additive effects in reducing EGFP-HDQ74 aggregation and toxicity and enhancing the clearance of soluble EGFP-HDQ74 and A53T α-synuclein, compared to single treatments with calpastatin or rapamycin (**Fig. 7e–h**). The clearance effect was assessed at early time points where no major reductions in the levels of mutant proteins were observed with single treatments. We have used a saturating dose of rapamycin[11]. However, cotreatment with calpastatin and verapamil (both acting through the same pathway) did not facilitate any further clearance of the aggregate-prone proteins at this early time point (data not shown).

Therapeutic potential in HD models

In order to test whether compounds acting via the pathway identified in this screen are potentially relevant to therapy, we first tested them in a *Drosophila* model of HD (see **Supplementary Methods** online). Flies expressing a mutant huntingtin fragment with 120Q in the photoreceptors exhibit photoreceptor degeneration that is not observed in flies expressing the wild-type protein with 23Q (ref. 44). The photoreceptor degeneration in 120Q flies is attenuated with drugs acting on L-type Ca^{2+} channels (verapamil) or on the cAMP arm of the pathway (clonidine) (**Supplementary Fig. 7a,b** online). Valproate (which induces autophagy by reducing IP_3 levels[11], among other activities that may be relevant to HD) also had protective effects (**Supplementary Fig. 7c**).

As verapamil, clonidine and valproate slowed this neurodegeneration phenotype to a similar extent as various histone deacetylase inhibitors that are being extensively investigated in HD[45,46], we next tested representative compounds acting on our putative pathway in a zebrafish HD model we have generated that expresses EGFP-tagged

huntingtin exon 1 with 71Q (EGFP-HDQ71) in the rod photoreceptors using the rhodopsin promoter. In this model, constructs with EGFP-HDQ71 form aggregates (which are not seen with EGFP-HDQ23 constructs) and induce a loss of rhodopsin expression that correlates with rod photoreceptor degeneration (**Fig. 8a** and **Supplementary Fig. 8a–c** online). Zebrafish EGFP-HDQ71 models treated with verapamil, calpastatin, clonidine and 2′5′ddA had significantly fewer aggregates (as with rapamycin) and substantially enhanced rhodospin expression compared to untreated fish, while aggregation was increased and rhodopsin expression was decreased with (±)-Bay K8644 (**Fig. 8a–d**).

DISCUSSION

Our compound screen has identified a pathway regulating autophagy that provides many possibilities for therapeutic intervention (**Fig. 8e**). Previous studies have shown that the clearance of mutant huntingtin exon 1 (both EGFP-tagged and hemagglutinin-tagged), mutant full-length huntingtin and A53T or A30P α-synuclein is largely mediated by autophagy[8,13,14,20]. Conversely, wild-type full-length or exon 1 huntingtin and wild-type α-synuclein have very low dependencies on autophagy for their clearance[8,14,20]. Consistent with these expectations, a range of autophagy-inducing drugs have no obvious effects on wild-type huntingtin exon 1 or wild-type α-synuclein clearance[10,14]. Similarly, the drugs acting on the pathway we have identified in this study have no obvious effects on the clearance of wild-type huntingtin exon 1 (EGFP-HDQ23) or wild-type α-synuclein (**Supplementary Fig. 2g,h**).

Our data suggest that raised cAMP levels act via Epac and PLC-ε to enhance calpain activity, which retards the clearance of autophagy substrates (**Fig. 2a,b,d–f**; **Fig. 4f**; **Fig. 6a–c**; **Supplementary Fig. 3b,d,f,j–l**; **Supplementary Fig. 4a–d**; **Supplementary Fig. 6b–e**). The $G_{s\alpha}$–Epac–PLC-ε–Ca^{2+} release pathway operates in neurons and neuronal cells[32,47]. Importantly, this pathway can also be inhibited in neuronal cells by G_i stimulation (as would occur with clonidine)[34]. Likewise, L-type Ca^{2+} channel agonists slow the clearance of mutant proteins by blocking autophagy through calpain activation (**Figs. 1a–c** and **3a–d**; **Supplementary Fig. 2a–c,e,f**). $G_{s\alpha}$ provides a link between these two pathways as it is activated following calpain cleavage, leading to increased cAMP levels (**Fig. 8e** and **Supplementary Fig. 6a,d,e**). Notably, autophagosome synthesis can be induced and mutant huntingtin aggregation can be substantially inhibited by genetic knockdown of $G_{s\alpha}$ (**Fig. 6d,e,g** and **Supplementary Fig. 6f**). To our knowledge, this is the first demonstration of the importance of the Epac pathway in autophagy regulation. Previous studies in yeast have focused on PKA, and many of the mammalian studies that implicated PKA were performed before the Epac pathway was discovered[48,49]. The validity of the Epac pathway is consistent with the known activities of four additional compounds we identified in our screen that inhibit A53T α-synuclein clearance and enhance EGFP-HDQ74 aggregation: FPL61476 (**30**) has Ca^{2+} channel agonist activity, quinine sulfate and tolazamide are ATP-sensitive K^+ channel antagonists, and rolipram (**31**) inhibits phophodiesterase 4 (leading to increased levels of cAMP) (**Supplementary Fig. 2e,f**).

It is possible that changes in IP_3 and Ca^{2+} levels may have additional effects on autophagy. These are considered in the context of previous literature in the **Supplementary Discussion** online, which also deals with issues of cell-type pathway specificity.

Our data provides a possible link between excitotoxicity, which results from increased Ca^{2+} entry into neurons via glutamate receptors, and enhanced intracytosolic protein aggregation due to impaired autophagy. Excitotoxicity is believed to contribute to a number of neurodegenerative diseases, including HD and Alzheimer's disease (AD)[6,7], and it is notable that the proteins that aggregate in many of these diseases are autophagy substrates[1,8,15]. Calpain inhibition of autophagy may also contribute to the link between β-amyloid toxicity (which may elevate cytosolic Ca^{2+} levels) and tau accumulation in AD, as insoluble tau accumulates when autophagy is blocked[15]. Finally, it is tempting to speculate that our data may also go some way to explaining why apoptosis and autophagy generally do not coexist, as many apoptotic (and necrotic) cell death processes are associated with, or stimulated by, raised cytosolic Ca^{2+} levels[50].

Calpain activation has been proposed to contribute to HD pathogenesis by promoting huntingtin cleavage; the toxicity of the HD mutation appears to be exposed or enhanced after cleavage[4,5]. As the huntingtin fragments we used are N-terminal to the calpain cleavage sites at residues 469 and 536 (**Supplementary Fig. 1a**), the cumulative data strongly argue that calpain inhibition will reduce mutant huntingtin fragment levels by impairing cleavage (production) and by enhancing degradation (**Fig. 4a–e**). In addition to these effects that result in lowered levels of the toxic protein, calpain inhibition may have other benefits in neurodegenerative diseases, including protection against cell death (**Fig. 4a,b**).

Our data suggest that drugs acting on this mTOR-independent pathway may have added efficacy for neurodegenerative diseases in combination with rapamycin, providing a new direction for combinatorial treatment of disorders like HD by enhancing autophagy through two different routes (**Fig. 7e–h** and **Supplementary Fig. 6i,j**). Combination therapy with more moderate calpain and mTOR inhibition may be safer for long-term treatment compared to using higher doses of either compound, which results in more severe inhibition of a single pathway. This strategy may allow a larger safety window before toxic effects from non-autophagy-related effects of each drug are seen.

The discovery that autophagy induction can be mediated by Ca^{2+} channel blockers is particularly noteworthy, as these drugs are safer and better tolerated than rapamycin—for instance, verapamil has been used for decades to treat hypertension with minimal side effects. Our findings may have broad applicability, as autophagy appears to regulate the clearance of a range of intracytosolic aggregate-prone proteins associated with neurodegeneration and various intracellular bacteria[1].

METHODS

Screen design. We screened for autophagy enhancers using a library of 253 compounds that had previously been used in humans without major toxic side effects, and pharmacological probes.

We first assayed clearance of A30P α-synuclein, a well-characterized autophagy substrate[14], in stable inducible PC12 (neuronal precursor) cells. A30P and A53T α-synuclein are not substrates for chaperone-mediated autophagy[20]. Though these mutants are also dependent on the ubiquitin-proteasome system for their clearance, we have found these proteins to be excellent reporters for changes in autophagic activity through both mTOR-dependent and mTOR-independent pathways[10–12,14]. Autophagy inducers enhance A30P and A53T α-synuclein clearance, resulting in lower levels of the transgene, which is readily detectable after a 24-h switch-off period compared to the control. Conversely, clearance is retarded when autophagy is blocked, leading to higher levels of the transgene compared to control after the 24-h switch-off period. All compounds that visibly perturbed A30P α-synuclein clearance were retested and successfully validated in similar stable inducible PC12 cell lines expressing A53T α-synuclein.

Clearance of mutant huntingtin and A53T α-synuclein. Stable inducible PC12 cell lines expressing EGFP-HDQ74, or α-synuclein mutants (A53T or A30P), were induced with 1 μg ml^{-1} doxycycline (Sigma) for 8 h and 48 h,

respectively[8,14]. Transgene expression was switched off by removing doxycycline from the medium. Cells were treated with or without compounds for time points as indicated in experiments. If transgene levels are followed at various times after switching off expression after an initial induction period, the effect of different drugs on transgene clearance can be assessed, as transgene expression decays when synthesis is stopped. Compounds were replenished every 24 h for EGFP-HDQ74 clearance. Clearance of soluble mutant huntingtin or α-synuclein mutants was detected with anti-EGFP or anti-hemagglutinin antibody, respectively.

Autophagy methods. We assessed autophagy by EGFP-LC3 vesicles as follows: the percentage of EGFP-positive cells with >5 EGFP-LC3 vesicles was counted, as previously described[11]. We assessed autophagy by LC3-II levels as follows: LC3-II levels, which directly correlate with autophagosome numbers[23,24], are detected with anti-LC3 antibody (NB100-2220, Novus Biologicals) and densitometry analysis relative to actin or tubulin. To see whether accumulation of LC3-II is due to increased autophagosome formation or impaired autophagosome-lysosome fusion, LC3-II is assessed in the presence of bafilomycin A1, which blocks autophagosome-lysosome fusion[39], as shown previously[10,12].

Other methods. See **Supplementary Methods** for details of plasmids; compounds; mammalian cell lines, culture and transfection; quantification and analysis of aggregate formation and cell death; assessment of autophagy by LC3; analysis of autophagosome-lysosome fusion; immunocytochemistry; western blot analysis; measurement of stored intracellular Ca^{2+}; RNA interference; assay for cAMP levels; Rap2B activation assay; electron microscopy; *Drosophila* analysis; and zebrafish analysis.

Statistical analysis by odds ratio. Pooled estimates for the changes in aggregate formation, cell death or EGFP-LC3 vesicles, resulting from perturbations assessed in multiple experiments, were calculated as odds ratios with 95% confidence intervals[8,11,12]. Odds ratios and P values were determined by unconditional logistical regression analysis, using the general log-linear analysis option of SPSS 9 software (SPSS). $^{***}P < 0.001$; $^{**}P < 0.01$; $^{*}P < 0.05$; NS, nonsignificant.

Statistical analysis on immunoblots. Densitometry analysis on the immunoblots was done by Scion Image Beta 4.02 software (Scion Corporation) from three independent experiments ($n = 3$). Significance for the clearance of mutant proteins was determined by factorial ANOVA test using STATVIEW software, version 4.53 (Abacus Concepts). The control condition was set to 100%, and the error bars denote s.e.m.

Note: Supplementary information and chemical compound information is available on the Nature Chemical Biology website.

ACKNOWLEDGMENTS

We thank T. Yoshimori (Osaka University) for LC3 antibody, myc-LC3 and EGFP-LC3 constructs, N. Mizushima (Tokyo Medical and Dental University) for wild-type and knockout *Atg5* MEFs, wild-type Atg5 and K130R Atg5 constructs, G. Jackson (University of California, Los Angeles) for the *gmrQ120* flies, K.L. Guan (University of Michigan, Ann Arbor) for rheb construct, A. Wells (University of Pittsburgh) for constitutive active S50E m-calpain construct, J. Lomasney (Northwestern University, Chicago) for wild-type PLC-ε construct, J. de Gunzburg (Institut Curie, Paris) for dominant-negative Rap2B construct, R.F. Irvine (University of Cambridge) for cytosolic IP_3 kinase A construct, M. Mizuguchi (Toyama Medical and Pharmaceutical University) for human LC3B construct, J.P. Luzio (University of Cambridge) for GFP-lgp20 construct, R. Tsien (University of California, San Diego) for mCherry construct, A.M. Tolkovsky (University of Cambridge) for EGFP-LC3 HeLa stable cells, N.P. Dantuma (Karolinska Institute, Stockholm) for Ub^{G76V}-GFP HeLa stable cells, M. Mahaut-Smith for use of the spectrophotometer, J.N. Skepper for EM, A. Roach for critical comments and A. Cordenier for technical assistance. We are grateful for the Gates Cambridge Scholarship and Hughes Hall Research Fellowship (S. Sarkar), Medical Research Council Studentships (A.W., E.K.T.), Biotechnology and Biological Sciences Research Council Career Development Award (C.J.O.'K.), Eli Lilly Pergolide Fellowship (S. Saiki), Academy of Medical Sciences–Medical Research Council Clinical Scientist Fellowship (R.A.F.), Wellcome Trust Senior Fellowship in Clinical Science (D.C.R.), Knowledge Transfer Partnership grant (Department of Trade and Industry), an MRC Programme Grant, an MRC Link Grant, European Union Framework VI (EUROSCA) and the National Institute for Health Research Biomedical Research Centre at Addenbrooke's Hospital for funding.

AUTHOR CONTRIBUTIONS

A.W., S. Sarkar, P.C., E.K.T., S. Saiki, F.H.S., L.J., D.P. and R.A.F. performed experiments. All authors participated in the design and analysis of various experiments. A.W., S. Sarkar and D.C.R. wrote the paper.

COMPETING INTERESTS STATEMENT

The authors declare competing financial interests: details accompany the full-text HTML version of the paper at http://www.nature.com/naturechemicalbiology/.

Published online at http://www.nature.com/naturechemicalbiology
Reprints and permissions information is available online at http://npg.nature.com/reprintsandpermissions

1. Rubinsztein, D.C., Gestwicki, J.E., Murphy, L.O. & Klionsky, D.J. Potential therapeutic applications of autophagy. *Nat. Rev. Drug Discov.* **6**, 304–312 (2007).
2. Klionsky, D.J. & Emr, S.D. Autophagy as a regulated pathway of cellular degradation. *Science* **290**, 1717–1721 (2000).
3. Rubinsztein, D.C. Lessons from animal models of Huntington's disease. *Trends Genet.* **18**, 202–209 (2002).
4. Gafni, J. & Ellerby, L.M. Calpain activation in Huntington's disease. *J. Neurosci.* **22**, 4842–4849 (2002).
5. Gafni, J. *et al.* Inhibition of calpain cleavage of huntingtin reduces toxicity: accumulation of calpain/caspase fragments in the nucleus. *J. Biol. Chem.* **279**, 20211–20220 (2004).
6. Zeron, M.M. *et al.* Increased sensitivity to N-methyl-D-aspartate receptor-mediated excitotoxicity in a mouse model of Huntington's disease. *Neuron* **33**, 849–860 (2002).
7. Tang, T.S. *et al.* Huntingtin and huntingtin-associated protein 1 influence neuronal calcium signaling mediated by inositol-(1,4,5) triphosphate receptor type 1. *Neuron* **39**, 227–239 (2003).
8. Ravikumar, B., Duden, R. & Rubinsztein, D.C. Aggregate-prone proteins with polyglutamine and polyalanine expansions are degraded by autophagy. *Hum. Mol. Genet.* **11**, 1107–1117 (2002).
9. Ravikumar, B. *et al.* Inhibition of mTOR induces autophagy and reduces toxicity of polyglutamine expansions in fly and mouse models of Huntington disease. *Nat. Genet.* **36**, 585–595 (2004).
10. Sarkar, S., Davies, J.E., Huang, Z., Tunnacliffe, A. & Rubinsztein, D.C. Trehalose, a novel mTOR-independent autophagy enhancer, accelerates the clearance of mutant huntingtin and alpha-synuclein. *J. Biol. Chem.* **282**, 5641–5652 (2007).
11. Sarkar, S. *et al.* Lithium induces autophagy by inhibiting inositol monophosphatase. *J. Cell Biol.* **170**, 1101–1111 (2005).
12. Sarkar, S. *et al.* Small molecules enhance autophagy and reduce toxicity in Huntington's disease models. *Nat. Chem. Biol.* **3**, 331–338 (2007).
13. Shibata, M. *et al.* Regulation of intracellular accumulation of mutant Huntingtin by Beclin 1. *J. Biol. Chem.* **281**, 14474–14485 (2006).
14. Webb, J.L., Ravikumar, B., Atkins, J., Skepper, J.N. & Rubinsztein, D.C. Alpha-Synuclein is degraded by both autophagy and the proteasome. *J. Biol. Chem.* **278**, 25009–25013 (2003).
15. Berger, Z. *et al.* Rapamycin alleviates toxicity of different aggregate-prone proteins. *Hum. Mol. Genet.* **15**, 433–442 (2006).
16. Gutierrez, M.G. *et al.* Autophagy is a defense mechanism inhibiting BCG and *Mycobacterium tuberculosis* survival in infected macrophages. *Cell* **119**, 753–766 (2004).
17. Nakagawa, I. *et al.* Autophagy defends cells against invading group A Streptococcus. *Science* **306**, 1037–1040 (2004).
18. Ogawa, M. *et al.* Escape of intracellular Shigella from autophagy. *Science* **307**, 727–731 (2005).
19. Sarbassov, D.D., Ali, S.M. & Sabatini, D.M. Growing roles for the mTOR pathway. *Curr. Opin. Cell Biol.* **17**, 596–603 (2005).
20. Cuervo, A.M., Stefanis, L., Fredenburg, R., Lansbury, P.T. & Sulzer, D. Impaired degradation of mutant alpha-synuclein by chaperone-mediated autophagy. *Science* **305**, 1292–1295 (2004).
21. Greenberg, D.A., Cooper, E.C. & Carpenter, C.L. Calcium channel 'agonist' BAY K 8644 inhibits calcium antagonist binding to brain and PC12 cell membranes. *Brain Res.* **305**, 365–368 (1984).
22. Hockerman, G.H., Peterson, B.Z., Johnson, B.D. & Catterall, W.A. Molecular determinants of drug binding and action on L-type calcium channels. *Annu. Rev. Pharmacol. Toxicol.* **37**, 361–396 (1997).
23. Mizushima, N. Methods for monitoring autophagy. *Int. J. Biochem. Cell Biol.* **36**, 2491–2502 (2004).
24. Kabeya, Y. *et al.* LC3, a mammalian homologue of yeast Apg8p, is localized in autophagosome membranes after processing. *EMBO J.* **19**, 5720–5728 (2000).
25. Osborne, N.N. Inhibition of cAMP production by alpha 2-adrenoceptor stimulation in rabbit retina. *Brain Res.* **553**, 84–88 (1991).
26. Felsen, D. *et al.* Identification, localization and functional analysis of imidazoline and alpha adrenergic receptors in canine prostate. *J. Pharmacol. Exp. Ther.* **268**, 1063–1071 (1994).

27. Greney, H. *et al.* Coupling of I(1) imidazoline receptors to the cAMP pathway: studies with a highly selective ligand, benazoline. *Mol. Pharmacol.* **57**, 1142–1151 (2000).
28. Kopperud, R., Krakstad, C., Selheim, F. & Doskeland, S.O. cAMP effector mechanisms. Novel twists for an 'old' signaling system. *FEBS Lett.* **546**, 121–126 (2003).
29. Kelley, G.G., Reks, S.E., Ondrako, J.M. & Smrcka, A.V. Phospholipase C(epsilon): a novel Ras effector. *EMBO J.* **20**, 743–754 (2001).
30. Enserink, J.M. *et al.* A novel Epac-specific cAMP analogue demonstrates independent regulation of Rap1 and ERK. *Nat. Cell Biol.* **4**, 901–906 (2002).
31. Shi, G.X., Rehmann, H. & Andres, D.A. A novel cyclic AMP-dependent Epac-Rit signaling pathway contributes to PACAP38-mediated neuronal differentiation. *Mol. Cell. Biol.* **26**, 9136–9147 (2006).
32. Ster, J. *et al.* Exchange protein activated by cAMP (Epac) mediates cAMP activation of p38 MAPK and modulation of Ca2+-dependent K+ channels in cerebellar neurons. *Proc. Natl. Acad. Sci. USA* **104**, 2519–2524 (2007).
33. Qiao, J., Mei, F.C., Popov, V.L., Vergara, L.A. & Cheng, X. Cell cycle-dependent subcellular localization of exchange factor directly activated by cAMP. *J. Biol. Chem.* **277**, 26581–26586 (2002).
34. vom Dorp, F. *et al.* Inhibition of phospholipase C-epsilon by Gi-coupled receptors. *Cell. Signal.* **16**, 921–928 (2004).
35. Criollo, A. *et al.* Regulation of autophagy by the inositol trisphosphate receptor. *Cell Death Differ.* **14**, 1029–1039 (2007).
36. Schell, M.J., Erneux, C. & Irvine, R.F. Inositol 1,4,5-trisphosphate 3-kinase A associates with F-actin and dendritic spines via its N terminus. *J. Biol. Chem.* **276**, 37537–37546 (2001).
37. Goll, D.E., Thompson, V.F., Li, H., Wei, W. & Cong, J. The calpain system. *Physiol. Rev.* **83**, 731–801 (2003).
38. Hayashi, S., Horie, M. & Okada, Y. Ionic mechanism of minoxidil sulfate-induced shortening of action potential durations in guinea pig ventricular myocytes. *J. Pharmacol. Exp. Ther.* **265**, 1527–1533 (1993).
39. Yamamoto, A. *et al.* Bafilomycin A1 prevents maturation of autophagic vacuoles by inhibiting fusion between autophagosomes and lysosomes in rat hepatoma cell line, H-4-II-E cells. *Cell Struct. Funct.* **23**, 33–42 (1998).
40. Ravikumar, B. *et al.* Dynein mutations impair autophagic clearance of aggregate-prone proteins. *Nat. Genet.* **37**, 771–776 (2005).
41. Gordon, P.B., Holen, I., Fosse, M., Rotnes, J.S. & Seglen, P.O. Dependence of hepatocytic autophagy on intracellularly sequestered calcium. *J. Biol. Chem.* **268**, 26107–26112 (1993).
42. Sato-Kusubata, K., Yajima, Y. & Kawashima, S. Persistent activation of Gsalpha through limited proteolysis by calpain. *Biochem. J.* **347**, 733–740 (2000).
43. Yousefi, S. *et al.* Calpain-mediated cleavage of Atg5 switches autophagy to apoptosis. *Nat. Cell Biol.* **8**, 1124–1132 (2006).
44. Jackson, G.R. *et al.* Polyglutamine-expanded human huntingtin transgenes induce degeneration of *Drosophila* photoreceptor neurons. *Neuron* **21**, 633–642 (1998).
45. Steffan, J.S. *et al.* Histone deacetylase inhibitors arrest polyglutamine-dependent neurodegeneration in *Drosophila*. *Nature* **413**, 739–743 (2001).
46. Butler, R. & Bates, G.P. Histone deacetylase inhibitors as therapeutics for polyglutamine disorders. *Nat. Rev. Neurosci.* **7**, 784–796 (2006).
47. Hucho, T.B., Dina, O.A. & Levine, J.D. Epac mediates a cAMP-to-PKC signaling in inflammatory pain: an isolectin B4(+) neuron-specific mechanism. *J. Neurosci.* **25**, 6119–6126 (2005).
48. Budovskaya, Y.V., Stephan, J.S., Reggiori, F., Klionsky, D.J. & Herman, P.K. The Ras/cAMP-dependent protein kinase signaling pathway regulates an early step of the autophagy process in *Saccharomyces cerevisiae*. *J. Biol. Chem.* **279**, 20663–20671 (2004).
49. Holen, I., Gordon, P.B., Stromhaug, P.E. & Seglen, P.O. Role of cAMP in the regulation of hepatocytic autophagy. *Eur. J. Biochem.* **236**, 163–170 (1996).
50. Orrenius, S., Zhivotovsky, B. & Nicotera, P. Regulation of cell death: the calcium-apoptosis link. *Nat. Rev. Mol. Cell Biol.* **4**, 552–565 (2003).